18. J. Dupuy *et al.*, *Structure* **14**, 129 (2006).
19. X. Brazzolotto, P. Timmins, Y. Dupont, J. M. Moulis, *J. Biol. Chem.* **277**, 11995 (2002).
20. C. C. Philpott, D. Haile, T. A. Rouault, R. D. Klausner, *J. Biol. Chem.* **268**, 17655 (1993).
21. H. Hirling, B. R. Henderson, L. C. Kühn, *EMBO J.* **13**, 453 (1994).
22. A. I. Selezneva, G. Cavigiolio, E. C. Theil, W. E. Walden, K. Volz, *Acta Crystallogr.* **F62**, 249 (2006).
23. J. P. Basilion, T. A. Rouault, C. M. Massinople, R. D. Klausner, W. H. Burgess, *Proc. Natl. Acad. Sci. U.S.A.* **91**, 574 (1994).
24. G. R. Swenson, W. E. Walden, *Nucleic Acids Res.* **22**, 2627 (1994).
25. P. Kaldy, E. Menotti, R. Moret, L. C. Kühn, *EMBO J.* **18**, 6073 (1999).
26. V. Gegout *et al.*, *J. Biol. Chem.* **274**, 15052 (1999).
27. C. C. Philpott, R. D. Klausner, T. A. Rouault, *Proc. Natl. Acad. Sci. U.S.A.* **91**, 7321 (1994).
28. S. Jones, D. T. Daley, N. M. Luscombe, H. M. Berman, J. M. Thornton, *Nucleic Acids Res.* **29**, 943 (2001).
29. Z. Kikinis, R. S. Eisenstein, A. J. Bettany, H. N. Munro, *Nucleic Acids Res.* **23**, 4190 (1995).
30. P. C. Haasnoot, J. F. Bol, R. C. Olsthoorn, *Proc. Natl. Acad. Sci. U.S.A.* **100**, 12596 (2003).
31. B. R. Henderson, E. Menotti, C. Bonnard, L. C. Kühn, *J. Biol. Chem.* **269**, 17481 (1994).
32. P. J. Beuning, K. Musier-Forsyth, *Biopolymers* **52**, 1 (1999).
33. R. Erlitzki, J. C. Long, E. C. Theil, *J. Biol. Chem.* **277**, 42579 (2002).
34. Y. Ke, E. C. Theil, *J. Biol. Chem.* **277**, 2373 (2002).
35. B. L. Gourley, S. B. Parker, B. J. Jones, K. B. Zumbrennen, E. A. Leibold, *J. Biol. Chem.* **278**, 3227 (2003).
36. Single-letter abbreviations for the amino acid residues are as follows: A, Ala; C, Cys; D, Asp; E, Glu; F, Phe; G, Gly; H, His; I, Ile; K, Lys; L, Leu; M, Met; N, Asn; P, Pro; Q, Gln; R, Arg; S, Ser; T, Thr; V, Val; W, Trp; and Y, Tyr.
37. QUANTA, 1997 (Molecular Simulations, Inc., San Diego, CA, 1997).
38. W. L. DeLano, *The PyMOL Molecular Graphics System* (DeLano Scientific, San Carlos, CA, 2002).

39. Supported by grants from the National Institutes of Health (DK47281 to W.E.W., DK20251 to E.C.T., and GM47522 to K.V.). We thank E. A. Craig, R. S. Eisenstein, H. Noller, T. A. Steitz, and D. S. Ucker for critical review of the manuscript. Data were collected at the Southeast regional collaborative access team (SER-CAT) 22-ID at the Advanced Photon Source, Argonne National Laboratory. Use of the Advanced Photon Source was supported by the Department of Energy under contract No. W-31-109-Eng-38. Structure factors and coordinates have been deposited in the Protein Data Bank (accession code 2IPY).

Supporting Online Material

www.sciencemag.org/cgi/content/full/314/5807/1903/DC1
Materials and Methods
Tables S1 and S2
References
Movies S1 and S2

27 July 2006; accepted 3 November 2006
10.1126/science.1133116

REPORTS

A Gaseous Metal Disk Around a White Dwarf

B. T. Gänsicke,* T. R. Marsh, J. Southworth, A. Rebassa-Mansergas

The destiny of planetary systems through the late evolution of their host stars is very uncertain. We report a metal-rich gas disk around a moderately hot and young white dwarf. A dynamical model of the double-peaked emission lines constrains the outer disk radius to just 1.2 solar radii. The likely origin of the disk is a tidally disrupted asteroid, which has been destabilized from its initial orbit at a distance of more than 1000 solar radii by the interaction with a relatively massive planetesimal object or a planet. The white dwarf mass of 0.77 solar mass implies that planetary systems may form around high-mass stars.

White dwarfs are the compact end products of stars with masses up to ~8 solar masses ($M_\odot$) (*1*). Because of the low luminosity of white dwarfs, the detection of low-mass stellar companions (*2*) or planets (*3*) is much easier around white dwarfs than around main-sequence stars. During a search for cool companions to white dwarfs, an excess infrared flux was discovered around the white dwarf G29-38 (*4*). The atmosphere of G29-38 has been found to be enriched with metals, i.e., elements heavier than helium. The sedimentation time scales of heavy elements in the high-gravity atmospheres of white dwarfs are short compared to the evolutionary time scale of these stars (*5*) and, hence, the high metal abundances in G29-38 imply that this star is accreting at a relatively high rate (*6*). Deep imaging and asteroseismological studies of G29-38 ruled out a brown dwarf companion (*7*, *8*) and led to the hypothesis of a cool dust cloud around the white dwarf. The presence of dust near G29-38 has been verified by infrared observations with the Spitzer Space Telescope (*9*). Infrared surveys of white dwarfs exhibiting metal-enriched atmospheres recently led to the discovery of three other potential dust disks (*10*–*12*). A possible origin of such dust disks is the tidal disruption of either comets (*13*) or asteroids (*14*). Asteroids appear to be more likely candidates because they can explain the large amount of metals accreted by the white dwarfs from the dusty environment, as well as the absence of hydrogen or helium. Although the detection of asteroid debris around G29-38 and the other white dwarfs represents a possible link to the existence of planetary systems around their main-sequence progenitor stars, modeling the excess infrared luminosity provides no direct information on the geometric location and extension of the dust, impeding a more detailed understanding of the nature and origin of the circumstellar material (*9*). A concentration of dust in the equatorial plane around G29-38 has been suggested on the basis of the relative amplitudes of non-radial white dwarf pulsations observed in the optical and infrared wavebands (*7*).

We identified SDSS J122859.93+104032.9 (henceforth SDSS 1228+1040) as a moderately hot white dwarf in the Data Release 4 of the Sloan Digital Sky Survey (SDSS) (*15*), but noted very unusual emission lines of the Ca II 850- to 866-nm triplet, as well as weaker emission lines of Fe II at 502 and 517 nm. The line profiles of the Ca II triplet display a distinct double-peaked morphology, which is the hallmark of a gaseous, rotating disk (*16*, *17*). Time-resolved spectroscopy (Fig. 1) and photometry do not reveal any radial velocity or brightness variations. These data exclude the possibility that SDSS 1228+1040 is an interacting white dwarf binary, in which an accretion disk around the white dwarf forms from material supplied by a nearby companion star. Furthermore, the absence of Balmer and helium emission lines implies that the gaseous disk around SDSS 1228+1040 must be extremely deficient in volatile elements, which independently rules out an interacting binary nature for this object.

Our detection of double-peaked metal emission lines from a circumstellar disk in SDSS 1228+1040 provides direct evidence for hydrogen- and helium-

Table 1. System parameter of SDSS 1228+1040. My, millions of years.

Distance	142 ± 15 pc
Effective temperature	22,020 ± 200 K
White dwarf mass	0.77 ± 0.02 $M_\odot$
White dwarf radius	0.0111 ± 0.0003 $R_\odot$
White dwarf cooling age	100 ± 5 My
Helium abundance	≤0.1 × solar
Calcium abundance	0.8 ± 0.15 × solar
Progenitor mass	4 to 5 $M_\odot$
Progenitor main-sequence life time	~ 70 My
Ca II full-width at zero intensity	1270 ± 35 km/s
Ca II peak separation	630 ± 5 km/s
Outer radius of the circumstellar disk	≅ 1.2 $R_\odot$
Ellipticity	0.021

Department of Physics, University of Warwick, Coventry CV4 7AL, UK.

*To whom correspondence should be addressed. E-mail: boris.gaensicke@warwick.ac.uk

depleted material rotating around a white dwarf at a very short distance in a flat, disklike structure. Assuming that the Ca II line profiles (Fig. 1) originate indeed in a circumstellar disk, it must have an azimuthal asymmetry to match the asymmetry in the profiles. Such asymmetries are known in the disks around B-type emission-line stars (Be stars) (*18*). Drawing upon this analogy, we developed a dynamical model of the Ca II line profiles [Fig. 2; supporting online material (SOM) text, section 1), which provides a robust constraint on the outer radius of the disk of ≅ 1.2 solar radii ($R_\odot$).

As the main-sequence stars hosting planetary systems evolve through the red-giant stage, they swell up and destroy planets and asteroids out to many hundred solar radii (*19*). The white dwarf mass of SDSS 1228+1040 implies a relatively massive main-sequence progenitor of ~ 4 to 5 $M_\odot$ (*20*), which will have expanded to a radius of ~1000 $R_\odot$ (*21*). It is therefore impossible that the material making up the present-day disk has survived the giant phase at its current location; it must instead have been brought inward from outside a distance of 1000 $R_\odot$. Planetary debris that migrated outward to large radii during the giant phase is expected to have relatively stable orbits unless perturbed by larger-mass objects (*13*). A likely scenario is therefore that one or more planets that survived the evolution of the progenitor of SDSS 1228+1040 destabilized the orbit of an asteroid sometime after the end of the planetary nebula phase. When it gets close enough to the compact star, the asteroid is tidally disrupted, forming a disk of metal-rich debris, which subsequently sublimates in the radiation field of the white dwarf. The radius derived from our dynamical model is indeed compatible with the tidal disruption radius for a rocky asteroid (*22*).

A strong Mg II 448-nm absorption line is detected in the spectrum of the white dwarf and implies a magnesium abundance in its atmosphere comparable to that of the Sun. This is extremely unusual for white dwarfs, which typically have pristine hydrogen atmospheres. The large abundance of magnesium can be explained only by sustained accretion, because the diffusion time scale for magnesium in a white dwarf atmosphere of 22,000 K (Fig. 3 and Table 1) is only ~5 days (*23*). Moreover, the accreted material must be of very low helium abundance, because small traces of helium already mixed into the radiative atmosphere of the white dwarf would cause noticeable He I 447-nm absorption, which is not observed. The absence of helium lines in the white dwarf spectrum places an upper limit on the helium abundance of the material accreted from the circumstellar disk of 0.1 times the solar value, which is independent evidence for a metal-rich composition of the disk around SDSS 1228+1040.

No infrared excess has been found around metal-polluted white dwarfs hotter than 15,000 K (*12*), which suggests that the radiation field of these hot white dwarfs causes sublimation of a dust disk. The case of SDSS 1228+1040 dem-

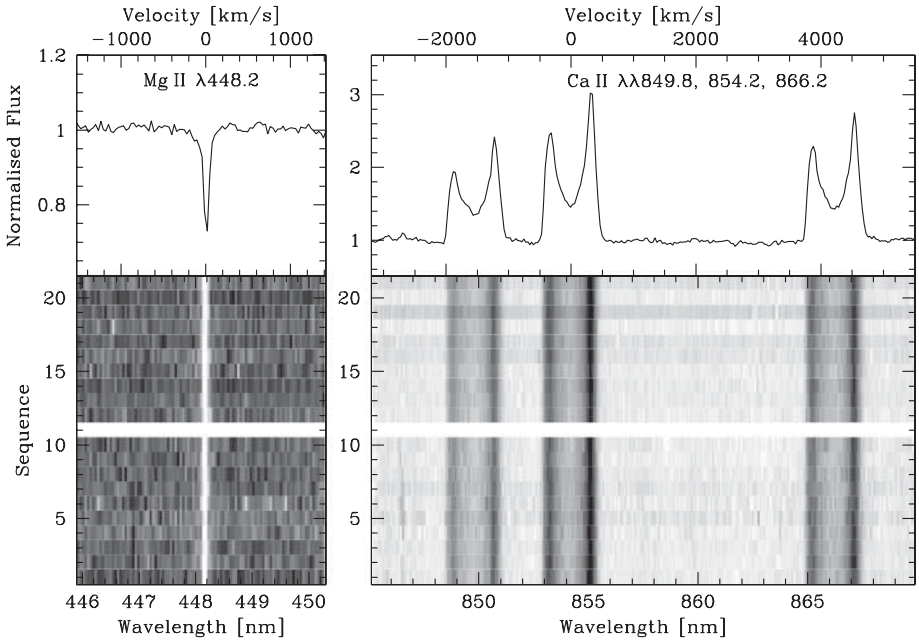

Fig. 1. Time-resolved spectroscopy of SDSS 1228+1040. Medium-resolution spectroscopy of SDSS 1228+1040 was obtained with the double-arm spectrograph ISIS on the 4.2-m William Herschel Telescope on La Palma, Canary Islands. Two sets of 10 consecutive spectra each were obtained on 30 June 2006 and 1 July 2006. The exposure times of the individual spectra were 600 s. The bottom panels show the two time series of spectra, each extending over 1.7 hours, centered on the calcium emission triplet (**right**) and the magnesium absorption line (**left**). The normalized average spectra are shown in the top panels. Radial velocities are given in the upper axes with respect to Ca II 854 nm (right) and Mg II 448 nm (left). The radial velocity of the Mg II line is stable to within ±4 km/s over time scales of 20 min to 1 day. Additional time-series photometry obtained at the Isaac Newton Telescope shows the star at constant brightness within ±0.01 mag.

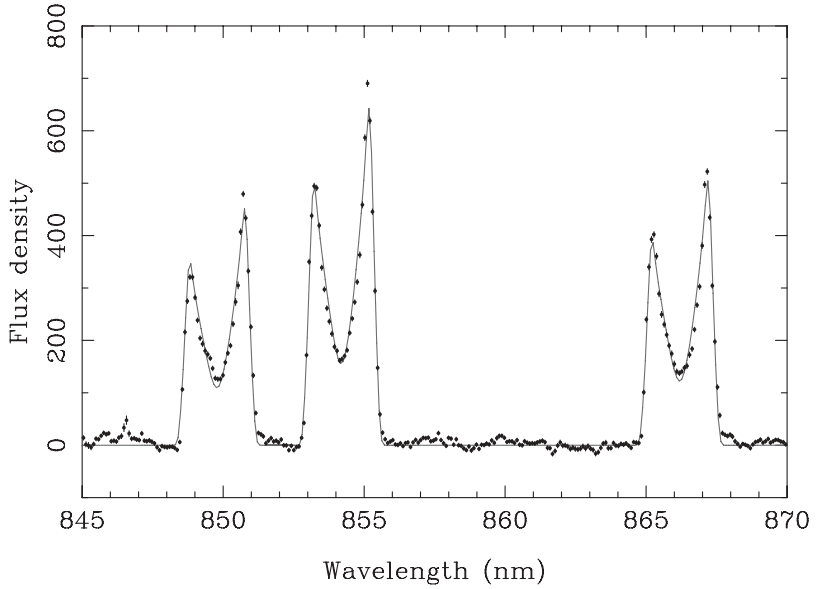

Fig. 2. A dynamical debris disk model. We modeled the observed Ca II emission line profiles (points) by assuming that the orbits in the disk took the form of a series of coaligned elliptical orbits of constant eccentricity (SOM text, section 1). We find an outer radius of 1.2 $R_\odot$ for an edge-on disk and an ellipticity of 0.021. The measured outer radius of the disk is relatively invulnerable to the detailed assumptions of the model because it is primarily fixed by the velocities of the emission-line peaks. The value given has to be interpreted as an upper limit because the radius scales as $\sin^2 i$ for disks inclined by angle i to the line of sight. The deep central dips of the profiles imply optically thick emission (*17*) and suggest that the orbital inclination must be quite high (>70°), and therefore the 1.2-$R_\odot$ upper limit should be close to the true value.

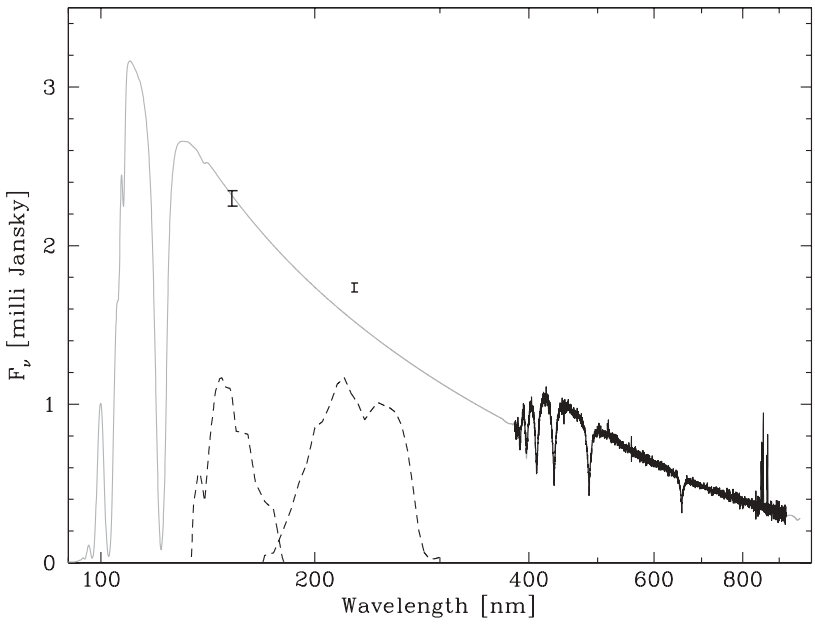

Fig. 3. A model of the white dwarf in SDSS 1228+1040. The optical SDSS spectrum of SDSS 1228+1040 is plotted in black. In addition to the Ca II emission lines seen in Fig. 1, Fe II 517 nm (and 502 nm, not visible at the plotted scale) is detected as well. The signal-to-noise ratio of the iron lines is too low to assess the shape of their profiles. The observed spectrum was modeled with synthetic white dwarf spectra (*25*), resulting in an effective temperature of $T_{WD} = 22{,}020 \pm 120$ K, a surface gravity of $\log g = 8.24 \pm 0.04$, an abundance of Mg II of 0.8 ± 0.15 with respect to solar abundances, and a limit of $v \sin i \leq 20$ km/s on the rotation rate of the white dwarf. The best-fit white dwarf model is plotted in gray. The ultraviolet fluxes detected by Galaxy Evolution Explorer (GALEX; http://galex.stsci.edu/GR2/) are indicated as black error bars, and the filter transmission curves of GALEX are shown by dashed lines. The best-fit white dwarf model is consistent with the far-ultraviolet GALEX flux, but a flux excess is observed in the near-ultraviolet. A host of Fe II transitions lie within the near-ultraviolet bandpass (*6*) and could be in emission in SDSS 1228+1040, explaining the observed flux excess.

onstrates that planetary debris material can be detected around younger and hotter white dwarfs in the form of gaseous disks. Prompted by the discovery of SDSS 1228+1040, we have inspected 406 SDSS spectra of white dwarfs with hydrogen-dominated atmospheres brighter than 17.5 in the *g*-bandpass that are contained in the SDSS Data Release 4 (*24*), and we find just one additional object that potentially exhibits flux excess in the region of the Ca II triplet (SDSS J104341.53+085558.2, fig. S1), so SDSS 1228+1040 is clearly a rare object. The detection of a metal-rich debris disk around this relatively massive white dwarf indicates that the formation of planetary systems can take place also around short-lived massive stars.

References and Notes

1. P. D. Dobbie *et al.*, *Mon. Not. R. Astron. Soc.* **369**, 383 (2006).
2. J. Farihi, E. E. Becklin, B. Zuckerman, *Astrophys. J. Suppl.* **161**, 394 (2005).
3. M. R. Burleigh, F. J. Clarke, S. T. Hodgkin, *Mon. Not. R. Astron. Soc.* **331**, L41 (2002).
4. B. Zuckerman, E. E. Becklin, *Nature* **330**, 138 (1987).
5. C. Paquette, C. Pelletier, G. Fontaine, G. Michaud, *Astrophys. J. Suppl.* **61**, 177 (1986).
6. D. Koester, J. Provencal, H. L. Shipman, *Astron. Astrophys.* **320**, L57 (1997).
7. J. R. Graham, K. Matthews, G. Neugebauer, B. T. Soifer, *Astron. J.* **357**, 216 (1990).
8. M. J. Kuchner, C. D. Koresko, M. E. Brown, *Astrophys. J. Lett.* **508**, L81 (1998).
9. W. T. Reach *et al.*, *Astrophys. J. Lett.* **635**, L161 (2005).
10. E. E. Becklin *et al.*, *Astrophys. J. Lett.* **632**, L119 (2005).
11. M. Kilic, T. von Hippel, S. K. Leggett, D. E. Winget, *Astrophys. J. Lett.* **632**, L115 (2005).
12. M. Kilic, T. von Hippel, S. K. Leggett, D. E. Winget, *Astrophys. J.* **646**, 474 (2006).
13. J. H. Debes, S. Sigurdsson, *Astrophys. J.* **572**, 556 (2002).
14. M. Jura, *Astrophys. J. Lett.* **584**, L91 (2003).
15. J. K. Adelman-McCarthy *et al.*, *Astrophys. J. Suppl.* **162**, 38 (2006).
16. P. Young, D. P. Schneider, S. A. Shectman, *Astrophys. J.* **245**, 1035 (1981).
17. K. Horne, T. R. Marsh, *Mon. Not. R. Astron. Soc.* **218**, 761 (1986).
18. A. Meilland, P. Stee, J. Zorec, S. Kanaan, *Astron. Astrophys.* **455**, 953 (2006).
19. I.-J. Sackmann, A. I. Boothroyd, K. E. Kraemer, *Astrophys. J.* **418**, 457 (1993).
20. T. Blöcker, *Astron. Astrophys.* **299**, 755 (1995).
21. J. R. Hurley, O. R. Pols, C. A. Tout, *Mon. Not. R. Astron. Soc.* **315**, 543 (2000).
22. B. J. R. Davidsson, *Icarus* **142**, 525 (1999).
23. D. Koester, D. Wilken, *Astron. Astrophys.* **453**, 1051 (2006).
24. D. J. Eisenstein *et al.*, *Astrophys. J. Suppl.* **167**, 40 (2006); preprint available at http://arxiv.org/abs/astro-ph/0606700 (2006).
25. I. Hubeny, T. Lanz, *Astrophys. J.* **439**, 875 (1995).
26. B.T.G., T.R.M., J.S., and A.R.M. were supported by an Advanced Fellowship from the Particle Physics and Astronomy Research Council (PPARC), a Senior Research Fellowship, a postdoctoral grant, and a joint PPARC-IAC (Instituto de Astrofísica de Canarias) studentship. The observations were obtained at the Spanish Observatorio del Roque de los Muchachos, IAC, with the William Herschel Telescope and Isaac Newton Telescope. We thank P. Wheatley for constructive comments on the manuscript, D. Koester for discussions on diffusion time scales, and I. Hubeny for ongoing support of the TLUSTY/SYNSPEC codes. Funding for the SDSS and SDSS-II was provided by the Alfred P. Sloan Foundation, the participating institutions, NSF, the U.S. Department of Energy, NASA, the Japanese Monbukagakusho, the Max Planck Society, and the Higher Education Funding Council for England. The SDSS Web site is at www.sdss.org/.

Supporting Online Material

www.sciencemag.org/cgi/content/full/314/5807/1908/DC1
SOM Text
Fig. S1
References

12 September 2006; accepted 25 October 2006
10.1126/science.1135033

Distinct Fermi-Momentum–Dependent Energy Gaps in Deeply Underdoped Bi2212

Kiyohisa Tanaka,[1,2] W. S. Lee,[1] D. H. Lu,[1] A. Fujimori,[3] T. Fujii,[4] Risdiana,[5] I. Terasaki,[5] D. J. Scalapino,[6] T. P. Devereaux,[7,8] Z. Hussain,[2] Z.-X. Shen[1]*

We used angle-resolved photoemission spectroscopy applied to deeply underdoped cuprate superconductors $Bi_2Sr_2Ca_{(1-x)}Y_xCu_2O_8$ (Bi2212) to reveal the presence of two distinct energy gaps exhibiting different doping dependence. One gap, associated with the antinodal region where no coherent peak is observed, increased with underdoping, a behavior known for more than a decade and considered as the general gap behavior in the underdoped regime. The other gap, associated with the near-nodal regime where a coherent peak in the spectrum can be observed, did not increase with less doping, a behavior not previously observed in the single particle spectra. We propose a two-gap scenario in momentum space that is consistent with other experiments and may contain important information on the mechanism of high–transition temperature superconductivity.

The pseudogap phase of underdoped cuprates has proven to be an important region for discoveries and surprises in the field of high-transition temperature (T_c) superconductors (*1*). Early angle-resolved photoemission spectroscopy (ARPES) (*2*) and electron tunneling experi-